Molecular characterization of siderophore biosynthesis in *Paracoccidioides brasiliensis*

Marielle Garcia Silva[1,2†], Juliana Santana de Curcio[1†], Mirelle Garcia Silva-Bailão[1], Raisa Melo Lima[1], Mariana Vieira Tomazett[1], Aparecido Ferreira de Souza[1], Vanessa Rafaela Milhomem Cruz-Leite[1], Nicolau Sbaraini[3], Alexandre Melo Bailão[1], Fernando Rodrigues[4,5], Maristela Pereira[1], Relber Aguiar Gonçales[4,5] and Célia Maria de Almeida Soares[1*]

Abstract

Iron is an essential nutrient for all organisms. For pathogenic fungi, iron is essential for the success of infection. Thus, these organisms have developed high affinity iron uptake mechanisms to deal with metal deprivation imposed by the host. Siderophore production is one of the mechanisms that fungal pathogens employ for iron acquisition. *Paracoccidioides* spp. present orthologous genes encoding the enzymes necessary for the biosynthesis of hydroxamates, and plasma membrane proteins related to the transport of these molecules. All these genes are induced in iron deprivation. In addition, it has been observed that *Paracoccidioides* spp. are able to use siderophores to scavenge iron. Here we observed that addition of the xenosiderophore ferrioxamine B FOB) to *P. brasiliensis* culture medium results in repression (at RNA and protein levels) of the SidA, the first enzyme of the siderophore biosynthesis pathway. Furthermore, SidA activity was reduced in the presence of FOB, suggesting that *P. brasiliensis* blocks siderophores biosynthesis and can explore siderophores in the environment to scavenge iron. In order to support the importance of siderophores on *Paracoccidioides* sp. life and infection cycle, silenced mutants for the *sidA* gene were obtained by antisense RNA technology. The obtained *AsSidA* strains displayed decreased siderophore biosynthesis in iron deprivation conditions and reduced virulence to an invertebrate model.

Keywords: Iron, SidA, RNA interference

INTRODUCTION

Iron is an essential nutrient for growth and development of living organisms. Due to iron redox properties, this metal occurs in two oxidation states, ferrous ion (Fe^{+2}) and ferric ion (Fe^{+3}), which are influenced by pH and oxygen (Sanchez et al. 2017). Fe^{+2} spontaneously convert to Fe^{+3} in the presence of oxygen (Halliwell and Gutteridge 1984). Iron is indispensable for a variety of cellular processes such as respiration, although, the excess or incorrect storage of this metal by cells is harmful. The reduced form of iron (Fe^{+2}) catalyzes the production of reactive oxygen species (ROS) through the Fenton/Haber Weiss reaction (Halliwell and Gutteridge 1984; Haber and Weiss 1934). In this way, the maintenance of the homeostasis of this micronutrient is essential. Proper iron homeostasis is achieved through fine-tuned regulation of iron acquisition, use and storage (Ganz 2009).

Nutritional immunity (i.e., host deprivation of metals, such Fe, Cu, Mn and Zn) is an important mechanism employed by the host to control the development of pathogenic organisms, to overcome the low availability of iron imposed by the host, microorganisms developed high affinity mechanisms for iron uptake (Raymond et al. 2003). In fungal pathogens these mechanisms include: the reduction of Fe^{+3} to Fe^{+2}, the acquisition of the iron bound to the heme group, and the solubilization of Fe^{+3} promoted by siderophores (Kornitzer 2009; Bailão et al.

2012; Canessa and Larrondo 2013). The last strategy, also known as non-reductive iron uptake, is characterized by the use of siderophores, which are low molecular weight compounds that bind Fe^{+3} with high affinity making it available for consumption (Neilands 1993).

Fungal siderophore biosynthesis is well characterized in *Aspergillus fumigatus* (Blatzer et al. 2011; Schrettl et al. 2004; Schrettl et al. 2007) and internalization of the siderophore-iron complex is performed by Siderophore Iron Transporters (SIT), such as Sit, MirA, MirB and MirC, located on the cell surface, as described in *Candida glabrata* and *Aspergillus nidulans* (Nevitt and Thiele 2011; Haas 2003; Haas et al. 2003). Siderophores are also produced by fungi of the *Paracoccidioides* genus that cause paracoccidioidomycosis (PCM) (Restrepo 1985), a disease restricted to Latin America (San-Blas et al. 2002) with high rates in Brazil (Restrepo et al. 2001). *Paracoccidioides* spp. grow as mycelia in the environment and as yeast cells in host tissues (Restrepo 1985). After inhalation of conidia or mycelial propagules, these reach the pulmonary alveoli of the host and differentiate into yeast cells, thus initiating the infectious process (McEwen et al. 1987).

Fungi of the *Paracoccidioides* genus can use reductive (Fe^{+3} to Fe^{+2}) and siderophore uptake pathways to acquire iron under conditions of metal shortage (Silva et al. 2011; Silva-Bailao et al. 2014; Bailao et al. 2015). We have demonstrated that *Paracoccidioides* spp. present putative orthologue genes to those related to hydroxamate siderophore production (*sidA, sidF, sidC, sidD, SidH* and *sidI*) as well as siderophore uptake (*sit1, mirB* and *mirC*) (Silva et al. 2011; Silva-Bailao et al. 2014). All of them are up-regulated in iron restriction and, in such condition, hydroxamate siderophores are produced (Silva-Bailao et al. 2014, Parente et al. 2011). Furthermore, *Paracoccidioides* spp. can also explore siderophores from other organisms to scavenge iron, as dimerumic acid and ferrioxamine B (FOB). Additionally, prior exposure of *P. brasiliensis* to FOB increases fungus survival to phagocytosis by activated macrophages (Silva-Bailao et al. 2014).

Considering those findings, we sought to investigate the adaptation of *P. brasiliensis* after FOB exposure as well as the functional role of SidA, the first enzyme in the siderophore production, in this fungus. Moreover, knockdown strains for *sidA* were generated employing antisense RNA technology and *Agrobacterium tumefaciens*-mediated transformation (ATMT) (Almeida et al. 2007; Menino et al. 2012; Bailao et al. 2014). Notably, upon FOB exposure, *P. brasiliensis' sidA* was down regulated at transcriptional and translational levels, which was accompanied by reduced enzymatic activity. Furthermore, the knockdown of *sidA* (*AsSidA*) led to reduced siderophore production by *P. brasiliensis* and

decreased fungal virulence to *Tenebrio molitor* an invertebrate model, suggesting an essential role of siderophores in the infection cycle of *P. brasiliensis*.

MATERIAL AND METHODS

Ethics statement

Mouse manipulation was carried out in accordance with the ethical principles of animal research adopted by the Brazilian Society of Laboratory Animal Science and a Brazilian Federal Law 11.749 (October 2008). Male BALB/c mice aged between 6 to 8 weeks were purchased from the Animal house of the Instituto de Patologia Tropical e Saúde Pública – UFG and were maintained in the Animal Facilities at the Laboratório de Biologia Molecular, Universidade Federal de Goiás. Animal experimentation was approved by institutional Ethics Commission on Animal Use of the Universidade Federal de Goiás – UFG (reference number 089/17).

Strains and culture conditions

Yeast cells of *P. brasiliensis*, *Pb*18 (ATCC32069) were used in all the experiments. Cells were maintained in brain heart infusion (BHI) solid medium added of 4% (w/v) glucose for 4 days, at 36 °C. For experiments, cells were grown in liquid BHI for 72 h at 36 °C, 150 rpm, in order to reach the exponential growth phase (10^7 cells per ml). Afterward, the cells were centrifuged at 1200 x *g* for 10 min at 4 °C and washed twice with Phosphate Buffered Saline (PBS) 1X. Cells were then incubated in McVeigh/Morton liquid medium (MMcM) (Restrepo and Jimenez 1980) containing: 4% (w/v) glucose, 0.15% (w/v) KH_2PO_4, 0.05% (w/v) $MgSO_4.7H_2O$, 0.015% (w/v) $CaCl_2.2H_2O$, 0.2% (w/v) $(NH_4)_2SO_4$, 0.2% (w/v) L-asparagine, 0.02% (w/v) L-cystine, 1% (v/v) of vitamin supplement (0.006% [w/v] thiamine, 0.006% [w/v] niacin B3, 0.006% [w/v] Ca^{+2} pantothenate, 0.001% [w/v] inositol B7, 0.0001% [w/v] biotin B8, 0.001% [w/v] riboflavin, 0.01% [w/v] folic acid B9, 0.01% [w/v] choline chloride, 0.01% [w/v] pyridoxine) and 0.1% (v/v) of trace elements supplement (0.0057% [w/v] H_3BO_3, 0.0081% [w/v] $MnSO_4.14H_2O$, 0.0036% [w/v] $(NH_4)_6MO_7O_{24}.4H_2O$, 0.0157% [w/v] $CuSO_4.H_2O$, 0.1404% [w/v] $Fe(NH_4)_2(SO_4)_2.6H_2O$) (Restrepo and Jimenez 1980) supplemented with 50 μM of bathophenanthroline-disulfonic acid (BPS; Sigma-Aldrich, Germany), a ferrous iron-specific chelator, for 24 h at 36 °C with shaking at 150 rpm (Parente et al. 2011, Silva-Bailao et al. 2014). Cells were centrifuged and washed twice with PBS 1X and cell viability was determined using trypan blue. A total of 10^7 cells per mL were transferred to MMcM medium containing 50 μM of BPS or 10 μM of ferrioxamine B with iron loaded (FOB; Sigma-Aldrich, Saint louis, USA) (Silva-Bailao et al. 2014). Yeast cells were incubated at 36 °C for 6 and 24 h, 150 rpm. For culture in MMcM medium

Silva *et al. IMA Fungus*   (2020) 11:11

Page 3 of 14

all the glassware was acid treated to remove residual traces of iron (Cox 1994).

RNA extraction and quantitative real time PCR (RT-qPCR)

Total RNA extraction was accomplished using TRIzol (TRI Reagent, Sigma-Aldrich, St. Louis, MO) and mechanical cell rupture (Mini-Beadbeater – Biospec Products Inc., Bartlesville, OK). The mRNA was reverse-transcribed using Super-Script III First-Strand Synthesis SuperMix (Invitrogen, Life Technologies). qRT-PCR was performed employing a QuantStudio5 real-time PCR system (Applied Biosystems Inc.) and SYBER green PCR master mix was used in the reaction mixture (Applied Biosystems, Foster City, CA). The sequences of forward and reverse oligonucleotides are listed in (Additional file 1: Table S1). The data were normalized with the 28 kDa ribonucleoprotein (GenBank accession number XP_015701336). The relative expression levels of transcripts of interest were calculated using the standard curve method for relative quantification (Bookout et al. 2006).

L-ornithine-N^5-oxygenase enzymatic assay

The enzymatic activity of L-ornithine-N^5-oxygenase (SidA) was evaluated as previously described by Zhou et al. (1998) and Haas et al. (1999) with few modifications. Briefly, *P. brasiliensis* yeast cells were collected and suspended in 0.5 mM potassium phosphate buffer (pH 8.0). The suspension was transferred to tubes containing glass beads (425–600 μm) and submitted to vigorous mixing in a bead beater apparatus (BioSpec) for 5 cycles with intervals of 30 s on ice. The samples were centrifuged 10,000 x *g* for 15 min and the protein concentration in supernatants was determined with the (Bradford) reagent. To measure the enzymatic activity of SidA, equal amounts of proteins (50 μg) of both conditions, yeast cells incubated with (BPS) or (FOB), were used. The reaction mixture containing 40 μl of 0.5 mM potassium phosphate pH 8.0, 10 μl of 10 mM NADPH, 2 μl of 0.5 mM FAD, 50 μg of cell extract, 30 μl of 10 mM L-ornithine was incubated at 30 °C for 2 h and added of 100 μl of 0.2 M perchloric acid to stop the reaction. For control, the same amount of perchloric acid was added to one sample before incubation. The samples were centrifuged and the supernatants were used to determine the absorbance at 340 nm.

Molecular modeling of SidA

The amino acid sequence of the *P. brasiliensis* SidA (PADG_00097) was modeled with ITASSER algorithm (Yang and Zhang 2015) available at (https://zhanglab.ccmb.med.umich.edu/). To predict protonation states of the model, the PDB2PQR server (http://nbcr-222.ucsd.edu/pdb2pqr_2.0.0/) at pH 7 was used. Pymol visualizer

was used to perform the structural analysis (Rigsby and Parker 2016).

The MD simulation was performed by the GROMACS 4.5.5 package, using the AMBER force field (ff99SB-ILDM) in the presence of water TIP3P. The protein was subjected to the simulation of 100 ns, temperature of 300 K, pressure of 1 atm and time interval of 2 fentoseconds, without restriction of the conformation (Pronk et al. 2013).

Analysis of Clusters, Root Mean Square Deviation (RMSD) and Root Mean Square Fluctuations (RMSF) were performed using the software of the GROMACS package. The quality analysis and the Ramachandran diagram of the final MD model were performed using the MolProbity server (http://molprobity.biochem.duke.edu/) (Chen et al. 2010).

Heterologous expression of recombinant SidA

Primers used for amplification of *SidA* cDNA were listed in (Additional file 1: Table S1). The PCR product was sub cloned into the *Bam*HI/*Eco*RI sites of pGEX-4 T3 vector (GE Healthcare Life Sciences). Transformation of *Escherichia coli* Rosetta (DE3) was carried out using standard procedures. For protein expression, transformed cells were cultured in LB medium supplemented with ampicillin (100 μg/ml) for 16 h at 37 °C. The induction of the recombinant protein was performed by addition of Isopropyl β-D-1-thiogalactopyranoside (IPTG; Sigma-Aldrich, St Louis, MO, USA) at a final concentration of 1 mM for 2 h. The size and identity of the recombinant protein SidA (rSidA) was evaluated using SDS-PAGE and in-gel protein digestion (Rezende et al. 2011) followed by LC-MS/MS (Lima Pde et al. 2015).

Polyclonal antibodies production and immunoblotting assay

rSidA was used in the production of specific mouse polyclonal antibodies. Pre-immune sera were obtained and stored at – 20 °C. The rSidA was extracted from the SDS-PAGE polyacrylamide gel, and subsequently injected into mouse three times at 15 days intervals. The obtained sera were sampled and stored at – 20 °C.

A total of 40 μg of the protein extract was loaded on 12% SDS-PAGE, stained with (Coomassie Blue R) or transferred to Hybond ECL membrane (GE Healthcare) as described by Lima and colleagues (Lima Pde et al. 2015). Blocked membranes were incubated with anti-SidA polyclonal antibodies diluted 1:150 for 2 h. After incubation, the membrane was washed and incubated with anti-mouse secondary antibody alkaline phosphatase conjugated (1: 20000). The reaction was developed using 5-bromo-4-chloro-3-indolylphosphate/nitroblue tetrazolium (BCIP/ NBT). As a load control was employed anti-enolase polyclonal antibodies (Nogueira et al. 2010). The pixel intensity

of the bands was analyzed using the ImageJ 1.51 software (Schneider et al. 2012) and expressed as arbitrary units.

Extraction and digestion of proteins for nano-ESI-UPLC-MS^E acquisition

Protein extraction was performed by protocol described by Baeza and coleagues (Baeza et al. 2017). The protein concentration in the supernatant was determined using the Bradford reagent (Bradford 1976). Bovine serum albumin was used as a standard. Integrity of the proteins was verified using a 12% SDS-PAGE. A total of 150 μg of cytoplasmic protein was prepared for nanoUPLC-MS^E analysis, as previously described (Lima Pde et al. 2015; Murad et al. 2011). After digestion, the peptides were ressuspended in 30 μl of ultrapure water and subsequently purified in ZipTip C18 Pipette Tips (Millipore, MA, USA) and dried in a speed vacuum. The obtained peptides were suspended in 80 μl of a solution containing 20 mM of ammonium formate and 200 fmol/μL of PHB (MassPREP™ protein). After solubilization, peptides were transferred to a Waters Total Recovery vial (Waters Corporation, MA, USA). For separation of tryptic peptides, Nanoscale LC was performed using an ACQUITY UPLC® M-Class system (Waters Corporation, MA, USA) (Tomazett et al. 2019).

Data processing and protein identification

Data processing were performed as previously described (Lima Pde et al. 2015). In brief, for proteomic analyzes of the data obtained from the LC-MS^E, the ProteinLynx Global Server version 3.0.2 (Waters, Manchester, UK) was employed. The processed spectra were searched against *P. brasiliensis* (*Pb*18) protein sequences (https://www.uniprot.org/proteomes/). The protein identification criteria also included the detection of at least 2 fragment ions per peptide, 5 fragments per protein and the determination of at least 1 peptide per protein. A protein that showed a variance coefficient of 0.057 and that was detected in all replicates was used to normalize the protein expression levels in the samples (PADG_04570). Expression^E informatics v.3.0.2 was used for quantitative comparisons. The mathematical model used to calculate the ratios was part of the Expression^E algorithm inside the PLGS software from the Waters Corporation (Geromanos et al. 2009). The minimum repeat rate for each protein in all replicates was 2. Protein tables generated by ProteinLynx Global Server were merged, and the dynamic range of the experiment was calculated using the software program MassPivot v1.0.1. The data obtained by NanoUPLC-MS^E were subjected to in silico analysis to identify functional classification. For this analysis, it was used FungiDB-database (https://fungidb.org/fungidb/).

Construction and characterization of the *P. brasiliensis* SidA antisense-RNA strain

The functional evaluation of SidA was performed by antisense RNA technique, as described by Bailão and colleagues (Bailao et al. 2014) and Parente-Rocha et al. (2015). *A. tumefaciens* strain LBA 1100 was used for *P. brasiliensis* genetic transformation experiments. The cells from *A. tumefaciens* were cultured in induction medium (IM) for co-cultivation. Transformants were selected in BHI medium containing hygromycin 75 μg/mL (w/v) and randomly selected clones were confirmed for silencing by qRT- PCR. RNA extraction, cDNA synthesis and real-time PCR procedure were performed.

P. brasiliensis wild type (WT), empty vector (EV) and silenced for *sidA* gene (*AsSidA*) were cultured in liquid MMcM at 36 °C and 180 rpm in the presence of iron. Cell growth was evaluated by optical density at a wavelength of 600 nm every 24 h. Cell viability analysis was evaluated by staining with 1 μg/mL (wt/vol) propidium iodide (Sigma Aldrich). The samples were analyzed in a fluorescence microscope (Zeiss Axiocam MRc – Scope A1) (Zambuzzi-Carvalho et al. 2013).

Siderophore production assayed by chrome azurol (CAS)

Siderophore production was analyzed as described previously (Silva-Bailao et al. 2014). For the overlay CAS (O-CAS) assay, 10^6 yeast cells were grown in solid MMcM medium with no iron supplementation for 5 days. After that, 15 ml of CAS solution (Schwyn and Neilands 1987) were applied over the plates. The ternary complex Chrome Azurol S/Fe^{3+}/hexadecyltrimetyl ammonium bromide (HDTMA) acts as an indicator of siderophore production, since it is originally blue and turns orange in presence of siderophores (Perez-Miranda et al. 2007).

The percentage of siderophores production was also determined (Machuca and Milagres 2003). Briefly, 10^6 yeast cells were grown in MMcM liquid medium with no iron supplementation or with different concentrations of ammonium ferrous sulfate (2.5 μm, 5 μm, 10 μm and 30 μm). After 5 days of growth, the culture supernatants were collected by centrifugation at 10,000 x *g* for 1 min and 400 μl were incubated with the same volume of CAS liquid medium (Schwyn and Neilands 1987). The reference sample was prepared by adding 400 μL of sterile MMcM without iron or with different iron concentrations to 400 μL of CAS liquid medium. After 1 h of incubation at room temperature in the dark, the absorbance at 630 nm (Ultraspec 2000 UV/Visible Spectrophotometer Pharmacia Biotech) was determined. The percentage of siderophore activity was calculated by subtracting the sample absorbance values from the reference according to the following formula $[(Ar−As/Ar)] \times 100$, in which Ar means absorbance of reference and As absorbance of sample.

Standardization of *Tenebrio molitor* larvae as an infection model for *P. brasiliensis*

T. molitor larvae were acquired from a local supplier and maintained in oatmeal diet until experimentation. *P. brasiliensis* yeast cells were cultured in BHI as previously described, collected through centrifugation, washed three times with PBS 1X and resuspended in PBS. The cells were repeatedly passed through a 18-gauge needle coupled to a 5 mL syringe and later strained through a 40 μm nylon filter to obtain a homogenous cell suspension. The cells were counted with a hemocytometer and diluted to specific concentrations with PBS. Hemocoel injection was performed with a Hamilton syringe (Sigma-Aldrich) in *T. molitor* larvae weighing between 150 and 200 mg, showing light and uniform color and absence of pigmented spots. The infection was performed in the ventral part of the larva, in the second segment after the paws and the volume of cell suspension was 5 μL (e.g., harboring 1×10^5, 1×10^6 or 2×10^6 cells). The larvae were kept in Petri dishes at 37 °C. The number of dead larvae was evaluated every 24 h for 10 days and deceased larvae were removed from the plate. As a control, the larvae were inoculated under the same conditions described above with PBS 1X. The experiments were performed with a total of 30 larvae per group.

Evaluation of *AsSidA* virulence in *T. molitor* larvae

P. brasiliensis yeast cells of WT, EV and *AsSidA* mutants were cultured and prepared as previously described. The infection was performed as previously described, employing 2×10^6 cells. The larvae were kept in Petri plates at 37 °C and the amount of dead larvae was evaluated every 24 h for 10 days. As a control, the larvae were inoculated under the same conditions described above with PBS 1X. The experiments were performed with a total of 30 larvae per group.

Statistical analysis

Student's *t*-test was used for the statistical analysis of the following experiments, enzymatic activity, qRT-PCR, immunobloting analysis and siderophores production. The following *P* values: $p \le 0.0005$, $p \le 0.005$ and $p \le 0.05$ were considered statistically significant, for each cited experiments, respectively. For the experiments in *T. molitor* the GraphPad Prism 5 program was used to generate the survival curve (using the Kaplan – Meier method) and for statistical analysis (Logrank [Mantel-Cox]). *p* value < 0.05 was considered significant (de Souza et al. 2015; de Souza et al. 2018a, 2018b).

RESULTS

Molecular modeling of SidA demonstrates its interaction with substrates for the first step in siderophore biosynthesis

Although *P. brasiliensis* has orthologs for the all the components for siderophore biosynthesis, the functionality of this pathway still remains elusive. Therefore, we employ molecular modeling to describe in silico the structural characteristics of SidA and its possible ligands. The described SidA proteins harbor a conserved domain of the superfamily of oxygenases (Pfam 13,434; This domain is conserved in the putative SidA of *P. brasiliensis*) and require NADPH and FAD as cofactors. The crystallized protein with the most similar three-dimensional structure corresponds to *A. fumigatus* SidA, with 47% identity (PDBID: 4B63) (Franceschini et al. 2012; Krithika et al. 2006). Thus, molecular modeling of *P. brasiliensis* putative SidA was employed, in order to support and identify amino acid residues that hypothetically bind to FAD, NADPH and L-ornithine. The molecular modeling and three-dimensional structure comparison was based on *A. fumigatus* SidA (i.e, already crystallized protein; PDBID: 4B63) displaying 47% identity with *P. brasiliensis* putative SidA ortholog.

The (Additional file 2: Fig. S1 A) shows the alignment of *A. fumigatus* SidA (gray) and *P. brasiliensis* SidA (blue) showing a preserved site of interaction with L-ornithine, FAD and NADPH. The amino acid residues that interact with L-ornithine in *A. fumigatus* are LYS107, ASN323 and SER469, which in the *P. brasiliensis* model correspond to LYS88, ASN306 and SER448, respectively (Additional file 2: Fig. S1 B). The interaction between NADPH and FAD occurs through a triad of amino acids GLN102, VAL168 and ARG279 in the crystal of *A. fumigatus*, corresponding to GLN83, VAL149 and LYS262 in *P. brasiliensis* (Additional file 2: Fig. S1 C).

P. brasiliensis SidA was subjected to molecular dynamics (MD) simulation and the Clusters and RMSD analyzes showed that the equilibration phase started in 20 ns and stabilized in approximately 60 ns (Additional file 3: Fig. S2 A and B). Cluster 1 was the most relevant, as it remained between 20 ns until the end of the simulation, with no significant differences between the conformational models during this simulation period.

The quality parameters generated through clashscore and MolProbity showed high values for the model prior to MD 12.28 and 3.18, respectively. After the MD, the values were 0 and 1.28, respectively, showing a significant improvement in the quality of the structure, mainly considering the reduction of shocks between the atoms (Additional file 4: Table S2). In the Ramachandran diagrams (Additional file 3: Fig. S2 C and D) we observed a decrease in amino acid residues in non-permitted regions (according to the *phi* and *psi* angles).

The most flexible regions of *P. brasiliensis* SidA, according to the RMSF analysis, and the SidA pockets are shown (Additional file 3: Fig. S2 E and F). It is worth mentioning that the unstable regions highlighted in the RMSF do not correspond to the regions of the catalytic site. As the structural analyzes showed a high-quality for *P. brasiliensis* SidA model, this structure could be used for other structure-based approaches. Thus, the analysis

of the molecular structure, suggests that SidA binds to L-ornithine as a substrate, and this reaction depends on NADPH and FAD.

Expression and enzyme activity of SidA upon FOB exposure

Once the functionally of *P. brasiliensis* SidA was supported through molecular modelling, the effects of FOB treatment over *P. brasiliensis* was thorough examined. The transcript levels of *sidA* were evaluated in the presence of FOB. Notably, *sidA* transcripts were down regulated at 6 and 24 h in FOB condition when compared to to iron starvation condition (BPS) (Fig. 1a). Additionally, the enzymatic activity of SidA decreased in *P. brasiliensis* yeast cells grown in the presence of FOB (iron loaded siderophore) (Fig. 1b), poiting for a correlation between transcript levels and enzyme amount. The data strongly suggested that the presence of an exogenous siderophore represses the biosynthesis of endogenous siderophores, since the fungus can be using Fe^{3+} attached to the xeno-siderophore as an alternative iron source.

SidA recombinant protein and polyclonal antibodies production allows the identification of SidA in yeast cells

The levels of SidA in *P. brasiliensis* cells were evaluated by western blotting with antibodies raised against recombinant SidA (rSidA). *P. brasiliensis* SidA protein was expressed in *E. coli* Rosetta (DE3) and rendered a protein with molecular mass of 79.5 kDa, corresponding to 53.5 kDa of SidA fused to 26 kDa of GST-tag (Fig. 2a). Following induction with IPTG, polyacrylamide gel pieces containing the recombinant protein were subjected to in-gel protein digestion for
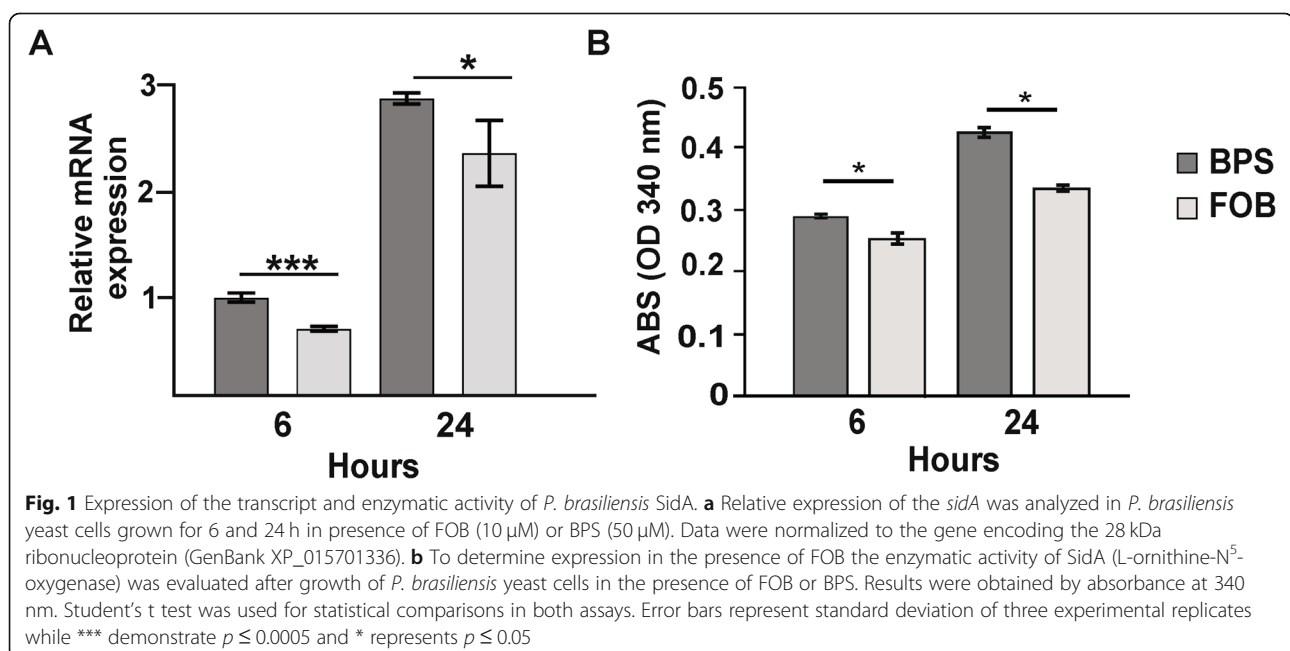
identification by LC-MS/MS approach; that confirmed the recombinant protein as SidA (Additional file 5: Fig. S3 and Additional file 6: Table S3). Immunoblotting results showed a decreased level of SidA in FOB-treated yeast cells when compared to BPS (Fig. 2b), corroborating the results obtained at transcript level. For loading control, membranes containing the same samples as in B were incubated with anti-*Pb*enolase polyclonal antibodies (Fig. 2c).

Label free proteomic analysis reveals that SidA is repressed in yeast cells grown in the presence of FOB

Proteomic analysis of *P. brasiliensis* yeast cells in presence of FOB and BPS was performed to evaluate alterations in the protein profile between both conditions. It was identified 431 and 475 proteins in BPS or FOB, respectively, in both time points, of 6 and 24 h (data not shown). Table 1 features the identified proteins, related to the synthesis of siderophores, which include those down and non-regulated. Proteins such as arginase (PADG_00637), ornithine aminotransferase (PADG_01328), glutamate-5-semialdehyde dehydrogenase (PADG_05337), NADP-specific glutamate dehydrogenase (PADG_04516), arginosuccinate synthase (PADG_00888), hydroxymethylglutaryl-CoA lyase (PADG_07031) and acetyl-CoA acetyltransferase (PADG_2751), which are related to the synthesis of ornithine, arginine and acetyl-CoA, respectively, were identified in the proteome. Notably, only SidA was down regulated after 24 h of incubation with FOB (Fig. 3 and Table 1).

Characterization of *sidA* silenced strains

The data obtained from gene expression, enzymatic activity, proteome and molecular modeling of SidA point to the function of this protein in *P. brasiliensis* as an

Fig. 1 Expression of the transcript and enzymatic activity of *P. brasiliensis* SidA. **a** Relative expression of the *sidA* was analyzed in *P. brasiliensis* yeast cells grown for 6 and 24 h in presence of FOB (10 μM) or BPS (50 μM). Data were normalized to the gene encoding the 28 kDa ribonucleoprotein (GenBank XP_015701336). **b** To determine expression in the presence of FOB the enzymatic activity of SidA (L-ornithine-N^5-oxygenase) was evaluated after growth of *P. brasiliensis* yeast cells in the presence of FOB or BPS. Results were obtained by absorbance at 340 nm. Student's t test was used for statistical comparisons in both assays. Error bars represent standard deviation of three experimental replicates while *** demonstrate $p \leq 0.0005$ and * represents $p \leq 0.05$

Fig. 2 Expression of the recombinant protein SidA and immunoblotting analysis. **a** SDS-PAGE of SidA expression by *E. coli* Rosetta (DE3). 79.5 kDa corresponds to 53.5 kDa of SidA fused to 26 kDa of GST-tag. **b** Membranes containing extracts of cytoplasmic proteins of *P. brasiliensis* cultivated in FOB or BPS for 24 h were incubated with pre-immune sera and anti-*Pb*SidA polyclonal antibodies. The native SidA protein presents a molecular mass of 53.5 kDa (black arrow). **c** Membranes with the same extracts described above were incubated with anti-*Pb*enolase polyclonal antibodies. The pixel intensity of the immunoblotting bands was analyzed using the ImageJ 1.51 software and expressed as arbitrary units. The Student's t test was used for statistical analysis. Error bars represent standard deviation of the experimental triplicate* $p \leq 0.05$. MW: molecular weight marker. P0: *E. coli* before IPTG induction. IND: *E. coli* after IPTG induction (1 mM IPTG for 2 h)

enzyme directly involved with the production of sidero-phores. Therefore, knockdown strains were constructed to determine the SidA role in *P. brasiliensis*. For that, it was used the antisense RNA technology, Fig. 4a depicts the *sidA* knockdown T-DNA cassette. This methodological approach provided *sidA*-knocked-down strains in *P. brasiliensis* yeast cells as demonstrated by qRT-PCR (Fig. 4b). The silencing percentage of six randomly selected clones ranged from 78 to 91% compared to those transformed with empty vector. *AsSidA* mutants grow similarly to the wild type and empty vector clones in MMcM medium supplemented with iron until 192 h. In addition, cells remained viable during the entire time growth (Fig. 4c).

sidA silenced strains present reduced siderophore production

Silenced clones were subjected to iron deprivation and subsequently subjected to O-CAS assay. As expected, in iron scarcity, WT and EV strains are still able to produce siderophores, while theknockdown strains (*AsSidA4* and *AsSidA5*) displayed a reduced production of these compounds (Fig. 5a). Furthermore, the siderophore production was evaluated in WT and *AsSidA5* strains after 5 days of growth in iron deprivation and in different iron concentrations (Fig. 5b). There was a pronounced decrease in sidero-phores production in *AsSidA5* strain in presence and absence of iron.

Table 1 Proteins related to the biosynthesis of siderophores identified in proteomic analysis

Accession number[a]	Description[b]	Time Point[c]	Score[d]
PADG_00637	Arginase (325 aa)	6 h	1131.29
PADG_00637	Arginase (325 aa)	24 h	1171.88
PADG_01328	Ornithine aminotransferase (461 aa)	6 h	2299.86
PADG_01328	Ornithine aminotransferase (461 aa)	24 h	1175.4
PADG_00888	Argininosuccinate synthase (416 aa)	6 h	3507.13
PADG_00888	Argininosuccinate synthase (416 aa)	24 h	4840.6
PADG_07031	Hydroxymethylglutaryl-CoA lyase (357 aa)	6 h	2406.52
PADG_07031	Hydroxymethylglutaryl-CoA lyase (357 aa)	24 h	2627.2
PADG_05337	Glutamate-5-semialdehyde dehydrogenase (457 aa)	6 h	1209.7
PADG_05337	Glutamate-5-semialdehyde dehydrogenase (457 aa)	24 h	771.05
PADG_04516	NADP-specific glutamate dehydrogenase (460 aa)	24 h	501.85
PADG_02751	Acetyl-CoA acetyltransferase (400 aa)	6 h	4328.06
PADG_02751	Acetyl-CoA acetyltransferase (400 aa)	24 h	3019.16
PADG_00097	L-ornithine-N^5-monooxigenase (475 aa)[e]	24 h	360.99

[a, b] Accession number and description of protein according to database of *Paracoccidioides* spp.(http://www.uniprot.proteomes/)
[c] Time of treatment with FOB
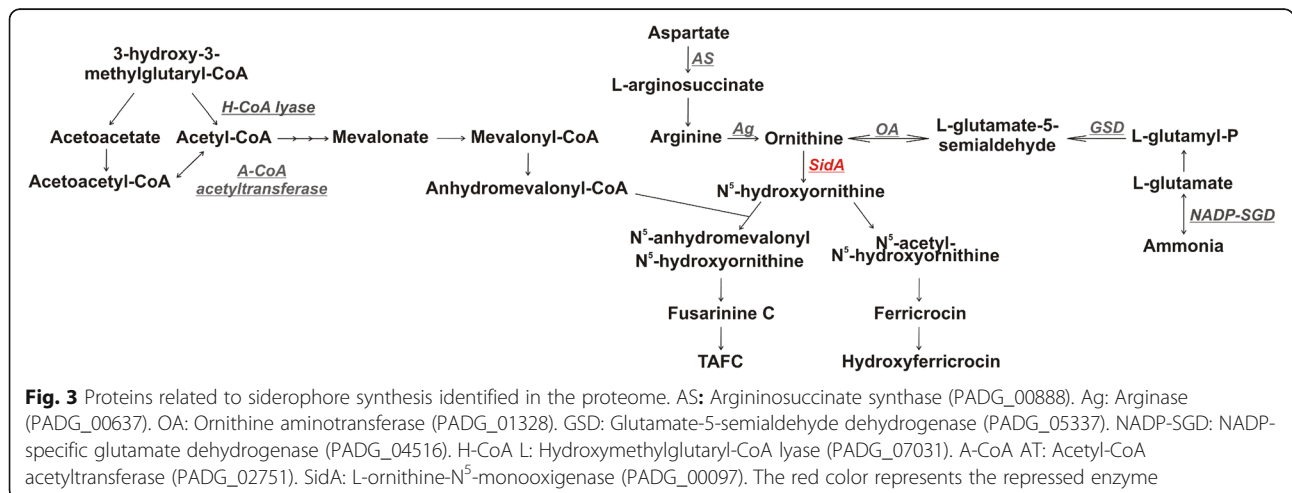[d] Protein score obtained from MS data using the PLGS
[e] Regulated Protein

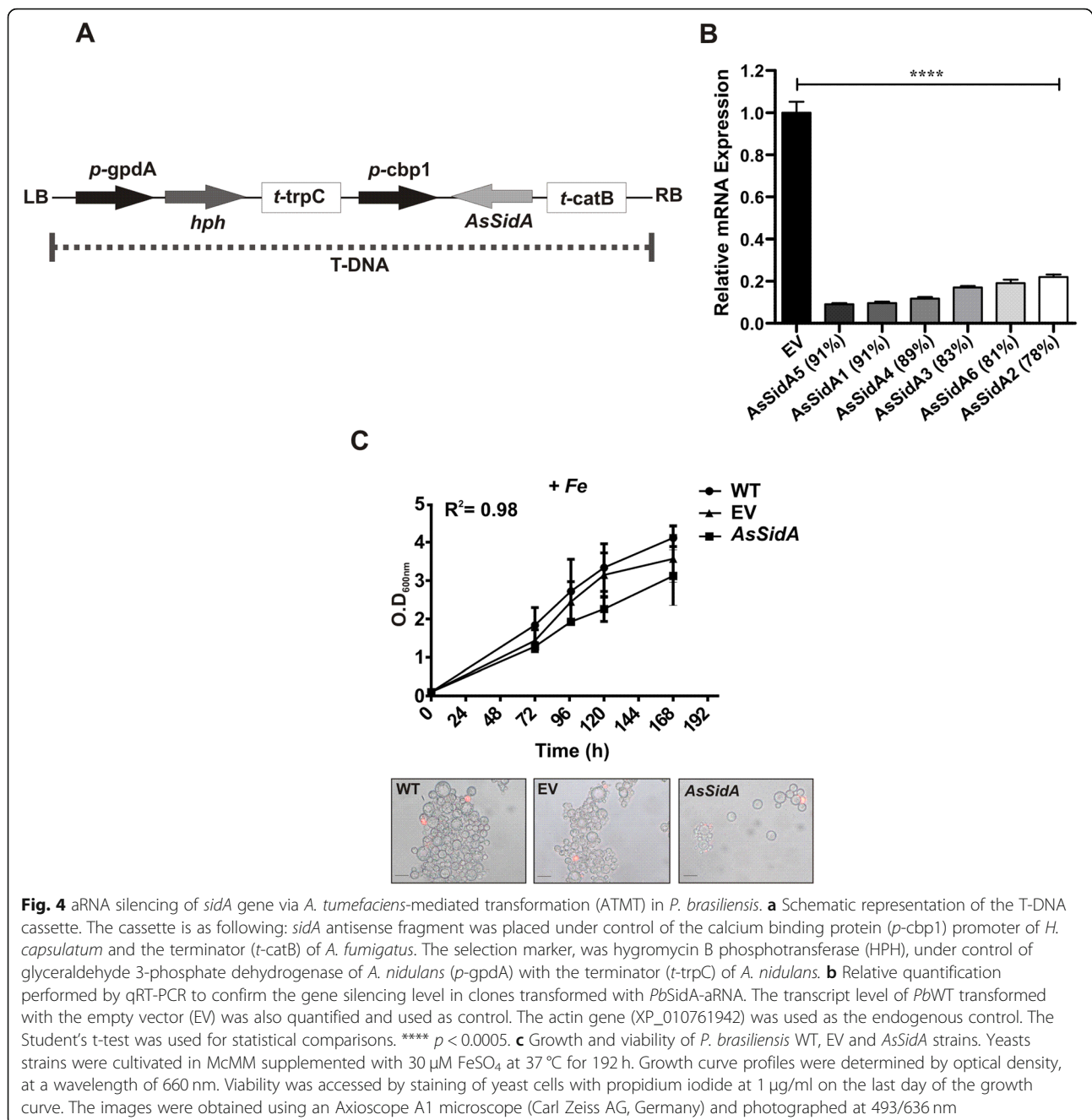### SidA can be a putative virulence factor in *P. brasiliensis*

Since it was the first virulence study of the effects of *P. brasiliensis* over *T. molitor* through intra-hemocoel injection, it was necessary to standardize the amount of cells needed to accomplish a successful infection in the larvae. First, only yeast cells of WT strain were employed to perform the standardization, followed by mutant analysis (EV and *AsSidA* strains). Thus, different concentrations of *P. brasiliensis* cells (1×10^5, 1×10^6 or 2×10^6) were inoculated in *T. molitor* larvae. As expected, larvae inoculated with *P. brasiliensis* cells showed an increase in the mortality rate as the fungus concentration also increased. The concentrations of 1×10^5 cells was not

enough to kill all *T. molitor* larvae, which showed a survival rate of 75% after 10 days of infection. Furthermore, 1×10^6 cells of *P. brasiliensis* were not able to kill all larvae, presenting a survival rate of 57% after 10 days. In light of these results, an ideal concentration of 2×10^6 cells was chosen. This concentration led to 100% mortality after 7 days post infection (Fig. 6a).

Once the ideal cell concentration was established, the ability of the *AsSidA* strains (*AsSidA4* and *AsSidA5*) to kill the *T. molitor* larvae was evaluated, comparing with WT and EV strains (Fig. 6b). Larvae infected with EV had a survival rate of only 4% after 10 days of infection, while larvae infected with *AsSidA* mutant strains had a

Fig. 3 Proteins related to siderophore synthesis identified in the proteome. AS: Argininosuccinate synthase (PADG_00888). Ag: Arginase (PADG_00637). OA: Ornithine aminotransferase (PADG_01328). GSD: Glutamate-5-semialdehyde dehydrogenase (PADG_05337). NADP-SGD: NADP-specific glutamate dehydrogenase (PADG_04516). H-CoA L: Hydroxymethylglutaryl-CoA lyase (PADG_07031). A-CoA AT: Acetyl-CoA acetyltransferase (PADG_02751). SidA: L-ornithine-N^5-monooxigenase (PADG_00097). The red color represents the repressed enzyme

Fig. 4 aRNA silencing of *sidA* gene via *A. tumefaciens*-mediated transformation (ATMT) in *P. brasiliensis*. **a** Schematic representation of the T-DNA cassette. The cassette is as following: *sidA* antisense fragment was placed under control of the calcium binding protein (*p*-cbp1) promoter of *H. capsulatum* and the terminator (*t*-catB) of *A. fumigatus*. The selection marker, was hygromycin B phosphotransferase (HPH), under control of glyceraldehyde 3-phosphate dehydrogenase of *A. nidulans* (*p*-gpdA) with the terminator (*t*-trpC) of *A. nidulans*. **b** Relative quantification performed by qRT-PCR to confirm the gene silencing level in clones transformed with *Pb*SidA-aRNA. The transcript level of *Pb*WT transformed with the empty vector (EV) was also quantified and used as control. The actin gene (XP_010761942) was used as the endogenous control. The Student's t-test was used for statistical comparisons. **** $p < 0.0005$. **c** Growth and viability of *P. brasiliensis* WT, EV and *AsSidA* strains. Yeasts strains were cultivated in McMM supplemented with 30 μM $FeSO_4$ at 37 ℃ for 192 h. Growth curve profiles were determined by optical density, at a wavelength of 660 nm. Viability was accessed by staining of yeast cells with propidium iodide at 1 μg/ml on the last day of the growth curve. The images were obtained using an Axioscope A1 microscope (Carl Zeiss AG, Germany) and photographed at 493/636 nm
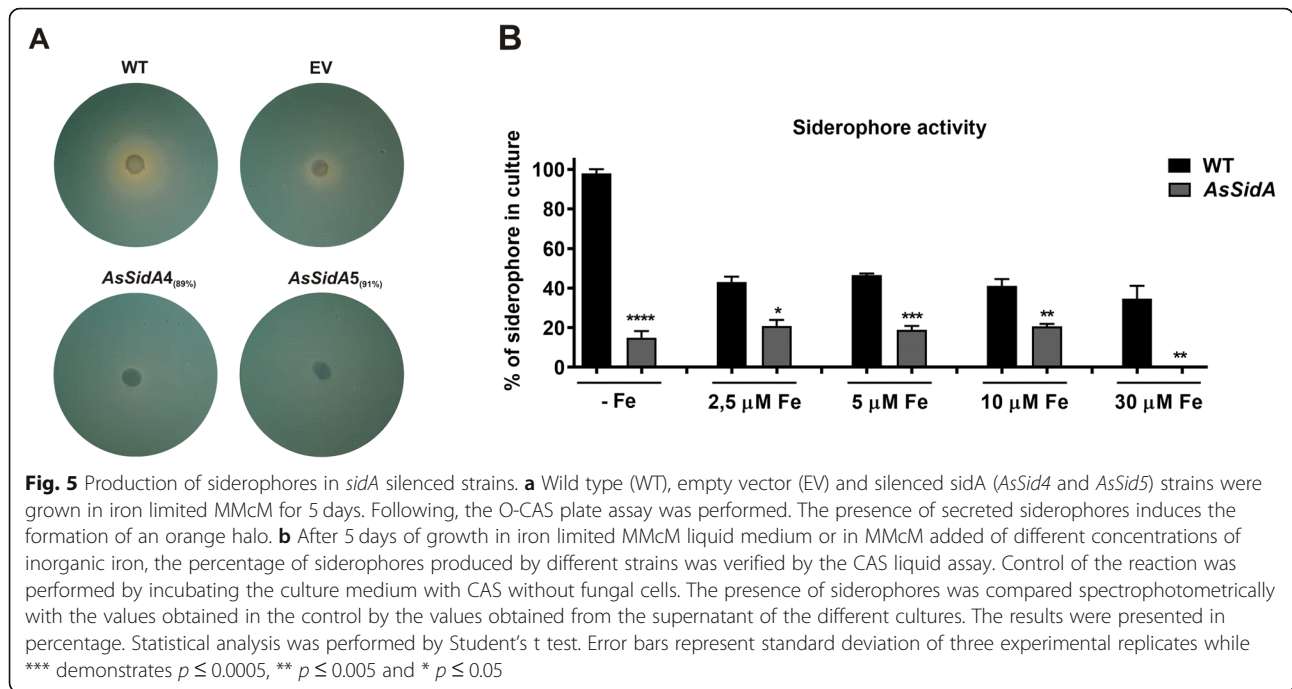
statistically significant reduction in larvae mortality, with a survival rate of 16 and 18%, respectively. These results point that the silencing of *SidA* affects the pathogenesis of *P. brasiliensis*, further supporting the role of siderophores on *Paracoccidioides* infection process.
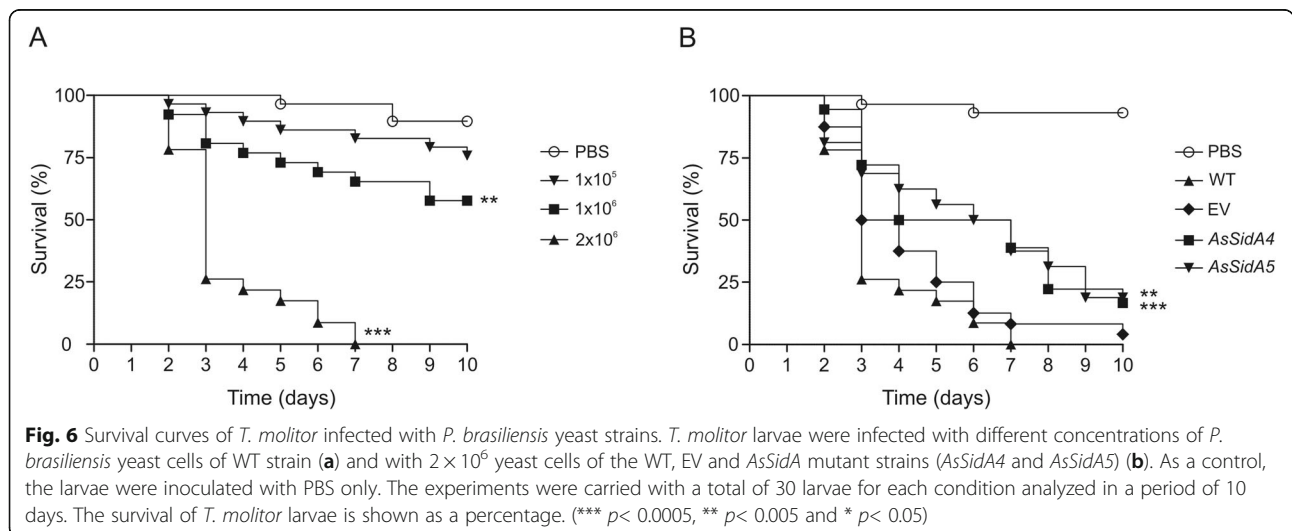
DISCUSSION

SidA is an enzyme specific for hydroxylation of ornithine, a precursor molecule of ferricrome siderophores biosynthesis (Chocklett and Sobrado 2010). The three-dimensional structure of SidA in *A. fumigatus* demonstrates the presence of amino acid residues essential for both NAPDH association and ornithine binding and hydroxylation (Robinson et al. 2015; Robinson et al. 2014). In this sense, SidA structure from *P. brasiliensis* was studied since the capacity of ornithine hydroxylation and use of NADPH as cofactor are specific to this enzyme (Chocklett and Sobrado 2010), which are influenced by the amino acids present in its structure (Robinson et al. 2014; Robinson et al. 2015). The characterization of the three-dimensional SidA structure of *P. brasiliensis* was performed by molecular modeling based on *A. fumigatus* crystal, which is most similar structure available (Sanchez

Silva *et al. IMA Fungus*   (2020) 11:11

Page 10 of 14

Fig. 5 Production of siderophores in *sidA* silenced strains. **a** Wild type (WT), empty vector (EV) and silenced sidA (*AsSid4* and *AsSid5*) strains were grown in iron limited MMcM for 5 days. Following, the O-CAS plate assay was performed. The presence of secreted siderophores induces the formation of an orange halo. **b** After 5 days of growth in iron limited MMcM liquid medium or in MMcM added of different concentrations of inorganic iron, the percentage of siderophores produced by different strains was verified by the CAS liquid assay. Control of the reaction was performed by incubating the culture medium with CAS without fungal cells. The presence of siderophores was compared spectrophotometrically with the values obtained in the control by the values obtained from the supernatant of the different cultures. The results were presented in percentage. Statistical analysis was performed by Student's t test. Error bars represent standard deviation of three experimental replicates while *** demonstrates $p \leq 0.0005$, ** $p \leq 0.005$ and * $p \leq 0.05$

et al. 2017). The amino acids from the active site ASN, SER and LYS coordinate L-ornithine in the pocket so that it can interact with NADPH and FAD. In *A. fumigatus*, mutations targeting residues in the L-ornithine binding site altered the substrate coupling and the kinetic parameters of the reaction. Among all mutations analyzed, alterations in LYS107, which corresponds to LYS88 in *P. brasiliensis*, led to important changes in the enzymatic kinetics and, therefore, it was considered the most important amino acid involved in enzymatic kinetics (Kosman 2003). Thus, molecular structure data confirm that the active site of *P. brasiliensis* SidA is conserved and has similar interaction residues when compared to *A. fumigatus* SidA.

We have previously demonstrated that members of the *Paracoccidioides* complex can use the heterologous siderophore ferrioxamine B (FOB) as an iron source and produce siderophores when grown in iron starvation conditions (Silva-Bailao et al. 2014). In an attempt to investigate the connection between siderophore biosynthesis and FOB utilization, experiments were conducted to demonstrate the repression of *sidA* when *P. brasiliensis* was incubated with FOB. In addition, SidA accumulation, at both transcriptional and proteomic level, and the cognate enzymatic activity were reduced in cells cultured in the presence of FOB, when compared to cells growing

Fig. 6 Survival curves of *T. molitor* infected with *P. brasiliensis* yeast strains. *T. molitor* larvae were infected with different concentrations of *P. brasiliensis* yeast cells of WT strain (**a**) and with 2×10^6 yeast cells of the WT, EV and AsSidA mutant strains (*AsSidA4* and *AsSidA5*) (**b**). As a control, the larvae were inoculated with PBS only. The experiments were carried with a total of 30 larvae for each condition analyzed in a period of 10 days. The survival of *T. molitor* larvae is shown as a percentage. (*** $p < 0.0005$, ** $p < 0.005$ and * $p < 0.05$)

in iron depleted medium. Similar results employing xenosiderophores were described for *Candida albicans*, *Saccharomyces cerevisiae* and *A. nidulans* (Heymann et al. 2002; Haas 2003; Philpott and Protchenko 2008).

In order to better explore the impact of FOB over *P. brasiliensis* growth a proteomic analysis was performed. Data allowed the identification of several proteins involved in siderophores biosynthesis. Notably, the decrease of SidA levels in presence of FOB was the most glaring result. Thus, all the data obtained in this study demonstrate that, in the presence of FOB, SidA is repressed both transcriptionally and translationally, and evidences the siderophore biosynthesis pathway in *P. brasiliensis*.

To confirm the function of SidA in the production of siderophores and the role of this protein in the biology of *P. brasiliensis*, we silenced the *sidA* gene by using antisense RNA technique. The same system was already reported to obtain *P. brasiliensis* silenced clones for proteins playing relevant roles in the fungal pathobiology, e.g., Cdc42p (Almeida et al. 2009), *Pb*HAD32 (Hernandez et al. 2010), *Pb*Rbt5 (Bailao et al. 2014), *Pb*ccp (Parente-Rocha et al. 2015), *Pb*14–3-3 (Marcos et al. 2016), and *Pb*PCN (Fernandes et al. 2017). Here we have successfully obtained knockdown strains for *PbsidA*, as demonstrated by qRT-PCR.

As silencing of *sidA* gene did not impair fungal growth in regular culture media, the phenotypic characterization of this gene was performed employing iron deprivation conditions. The qualitative O-CAS assay showed that production of siderophores in the knockdown strains was diminished when compared to the WT and EV strains. Furthermore, a semi-quantitative CAS liquid assay also highlighted the diminished production of siderophores with and without iron.

Although murine models are valuable tools for in vivo infection studies, invertebrate models are becoming prominent alternatives. The ethical reasons linked to vertebrate models, as well as the high costs for animal management have propelled the examination of viable substitutes (Wilson-Sanders 2011). Several studies have demonstrated the use of *Galleria mellonella* larvae to characterize the infection process in pathogenic fungi, such as *Histoplasma capsulatum*, *C. albicans*, *Cryptococcus neoformans* and *P. brasiliensis* (Thomaz et al. 2013; Vargas et al. 2015; Bouklas et al. 2015; Scorzoni et al. 2015; Marcos et al. 2019). However, *G. mellonella* is an animal that requires almost daily handling, as well as these insects are not sold worldwide (Jorjao et al. 2018). An alternative that has been explored are larvae of *T. molitor*, an animal that is easy to handle, is marketed by several suppliers and is a low cost insect. Furthermore, the *T. molitor* larvae have been standardized as an in vivo infection model for several fungal pathogens as *C. albicans*, *C. neoformans*, *Malassezia furfur* and *Fonsecaea pedrosoi* (de Souza et al. 2015; Silva et al. 2018; Fornari et al. 2018). Here, we explored the application of *T. molitor* as

an invertebrate infection model for *P. brasiliensis*. Noteworthy, increasing the viable cell concentration in the inoculum also increases *T. molitor* larvae mortality. The same observations can be draw for *C. albicans* and *C. neoformans*, demonstrating that this model is efficient for assessing the virulence of pathogenic fungi (de Souza et al. 2015).

Metal restriction is one of the several mechanisms employed by host cells to inhibit microbial development (Ganz 2016; Ganz 2018; Brechting and Rappleye 2019). Thus, the presence of a high affinity iron acquisition systems appears to be an essential strategy to circumvent the absence of this metal during growth in a hostile environment (McDonagh et al. 2008; Hilty et al. 2011; Pasricha et al. 2016; Kalidasan et al. 2018). In several fungal pathogens, siderophores are important for virulence and host-pathogen interaction (Heymann et al. 2002; Schrettl et al. 2004; Schrettl et al. 2010; Nevitt and Thiele 2011). For example, in *H. capsulatum*, the deletion of *sid1*, the homologue of *sidA* of *A. fumigatus*, promoted decreasing of siderophore production, resulting in diminished proliferation inside macrophages and murine pulmonary colonization (Hwang et al. 2008). Similarly, previous results pointed for a putative role of these molecules in pathogenesis of *P. brasiliensis*, since the expression of sidA was highly induced during fungal infection to macrophages (Silva-Bailao et al. 2014). The bioassays conducted here with *AsSidA* mutants support a main role of siderophores in the infection process of *Paracoccidioides* species. *AsSidA* mutants presented reduced virulence to *T. molitor* larvae, reasserting the importance of iron for host colonization.

CONCLUSIONS

Although previous results pointed that *P. brasiliensis* harbors a complete pathway for siderophore production several aspects about SidA regulation and activity were still to be determined. The molecular modelling, here employed, helped to highlight structural similarities between *A. fumigatus* SidA and *P. brasiliensis* SidA. Furthermore, the expression of SidA is repressed, at transcriptional and translational levels, in the presence of a xenosiderophore FOB. Moreover, *sidA* silencing in blocks the production of siderophores and promotes decrease in fungal virulence *P. brasiliensis*. Due to the relevance of iron for fungal survival inside the host, strategies aiming to block siderophore biosynthesis can be successful, helping to eliminate the infection. In this way, future studies will focus on molecules capable to block SidA activity.

Supplementary information

Additional file 1: Figure S1. Molecular structure of L–ornithine-N[5]-monooxygenase. (A) *Af*SidA from *Aspergillus fumigatus* PDBID: 4B63 (gray)

Silva *et al. IMA Fungus* (2020) 11:11

Page 12 of 14

and *Pb*SidA (blue) alignment using the Pymol viewer, evidencing the interactions among L-ornithine, FAD and NADPH. (B) Amino acid residues of *P. brasiliensis* SidA described as mainly involved in the interaction with L-ornithine and (C) cofactors are essential for the maintenance of them in the active site.

Additional file 2: Figure S2. Molecular dynamics of *P. brasiliensis* SidA. (A) Cluster and (B) RMSD graphs. It is observed that the stability starts at approximately 20 ns and that the most representative conformational mode of the trajectory is cluster 1. (C) Ramachandran diagrams of the three-dimensional model of SidA before molecular dynamics and (D) after molecular dynamics. (E) RMSF graph showing the more flexible residues (red) along the molecular dynamics. (F) Three-dimensional structure of SidA showing the most flexible regions (red) and pockets of the active site (green and orange).

Additional file 3: Figure S3. Characterization of the recombinant protein. MS/MS spectrum of the recombinant protein SidA identified by mass spectrometry.

Additional file 4: Table S1. Oligonucleotides used in this study.

Additional file 5: Table S2. Analysis of the quality of the SidA models through the Molprobity server.

Additional file 6: Table S3.

Authors' contributions
CMA Soares and MG Silva conceived and designed the experiments. MG Silva, JS de Curcio, MV Tomazett, AF Souza, VRMC Leite, RM Lima, N Sbaraini and RA Gonçales performed the experiments. MG Silva, JS de Curcio, MGS Bailão, AM Bailão, and CMA Soares analyzed and/or interpreted the data. M Pereira, F Rodrigues and CMA Soares contributed with reagents and materials. MG Silva, JS de Curcio, MGS Bailão and CMA Soares wrote the manuscript. The authors read and approved the final manuscript.

Availability of data and materials
Not applicable.

Ethics approval and consent to participate
All the animal work carried out in accordance with the ethical principles of animal research adopted by the Brazilian Society of Laboratory Animal Science and a Brazilian Federal Law 11.749 (October 2008).

Consent for publication
Not applicable.

Competing interests
The authors declare that they have no competing interests.

Author details
[1]Laboratório de Biologia Molecular, Instituto de Ciências Biológicas, ICB II, Campus II, Universidade Federal de Goiás, Goiânia, GO, Brazil. [2]Programa de Pós-graduação em Patologia Molecular, Faculdade de Medicina, Universidade de Brasília, Brasília, DF 70910-900, Brazil. [3]Centro de Biotecnologia, Programa de Pós-graduação em Biologia Celular e Molecular, Universidade Federal do Rio Grande do Sul, Porto Alegre, RS, Brazil. [4]Life and Health Sciences Research Institute (ICVS), School of Medicine, University of Minho, Braga, Portugal. [5]ICVS/3B's - PT Government Associate Laboratory, Braga/Guimarães, Portugal.

References
Almeida AJ, Carmona JA, Cunha C, Carvalho A, Rappleye CA, Goldman WE et al (2007) Towards a molecular genetic system for the pathogenic fungus *Paracoccidioides brasiliensis*. Fungal Genet Biol 44(12):1387–1398

Almeida AJ, Cunha C, Carmona JA, Sampaio-Marques B, Carvalho A, Malavazi I et al (2009) Cdc42p controls yeast-cell shape and virulence of *Paracoccidioides brasiliensis*. Fungal Genet Biol 46(12):919–926

Baeza LC, da Mata FR, Pigosso LL, Pereira M, de Souza G, Coelho ASG et al (2017) Differential metabolism of a two-carbon substrate by members of the *Paracoccidioides* genus. Front Microbiol 8:2308

Bailao EF, de Lima PS, Silva-Bailao MG, Bailao AM, Fernandes Gda R, Kosman DJ et al (2015) *Paracoccidioides* spp. ferrous and ferric iron assimilation pathways. Front Microbiol 6:821

Bailao EF, Parente JA, Pigosso LL, Castro KP, Fonseca FL, Silva-Bailao MG et al (2014) Hemoglobin uptake by *Paracoccidioides* spp. is receptor-mediated. PLoS Negl Trop Dis 8(5):e2856

Bailão EFLC, Parente AFA, Parente JA, Silva-Bailão MGS, Castro KP, Kmetzsch L et al (2012) Metal acquisition and homeostasis in fungi. Curr Fungal Infect Rep 6:257–266

Blatzer M, Schrettl M, Sarg B, Lindner HH, Pfaller K, Haas H (2011) SidL, an *Aspergillus fumigatus* transacetylase involved in biosynthesis of the siderophores ferricrocin and hydroxyferricrocin. Appl Environ Microbiol 77(14):4959–4966

Bookout AL, Cummins CL, Mangelsdorf DJ, Pesola JM, Kramer MF (2006) High-throughput real-time quantitative reverse transcription PCR. Curr Protoc Mol Biol Chapter 15(15.8):1–28

Bouklas T, Diago-Navarro E, Wang X, Fenster M, Fries BC (2015) Characterization of the virulence of *Cryptococcus neoformans* strains in an insect model. Virulence 6(8):809–813

Bradford MM (1976) A rapid and sensitive method for the quantitation of microgram quantities of protein utilizing the principle of protein-dye binding. Anal Biochem 72:248–254

Brechting PJ, Rappleye CA (2019) Histoplasma responses to nutritional immunity imposed by macrophage activation. J Fungi (Basel) 5(2):45

Canessa P, Larrondo LF (2013) Environmental responses and the control of iron homeostasis in fungal systems. Appl Microbiol Biotechnol 97(3):939–955

Chen VB, Arendall WB 3rd, Headd JJ, Keedy DA, Immormino RM, Kapral GJ et al (2010) MolProbity: all-atom structure validation for macromolecular crystallography. Acta Crystallogr D Biol Crystallogr 66(Pt 1):12–21

Chocklett SW, Sobrado P (2010) *Aspergillus fumigatus* SidA is a highly specific ornithine hydroxylase with bound flavin cofactor. Biochemistry 49(31):6777–6783

Cox CD (1994) Deferration of laboratory media and assays for ferric and ferrous ions. Methods Enzymol 235:315–329

de Souza P, Custodio Caloni C, Wilson D, Sergio Almeida R (2018) An invertebrate host to study fungal infections, mycotoxins and antifungal drugs: *Tenebrio molitor*. J Fungi (Basel) 4(4):125

de Souza PC, Morey AT, Castanheira GM, Bocate KP, Panagio LA, Ito FA et al (2015) *Tenebrio molitor* (Coleoptera: Tenebrionidae) as an alternative host to study fungal infections. J Microbiol Methods 118:182–186

Fernandes FF, Oliveira AF, Landgraf TN, Cunha C, Carvalho A, Vendruscolo PE et al (2017) Impact of Paracoccin gene silencing on *Paracoccidioides brasiliensis* virulence. MBio 8(4):e00537–e00517

Fornari G, Gomes RR, Degenhardt-Goldbach J, Dos Santos SS, de Almeida SR, Dos Santos GD et al (2018) A model for trans-kingdom pathogenicity in *Fonsecaea* agents of human Chromoblastomycosis. Front Microbiol 9:2211

Silva *et al. IMA Fungus*   (2020) 11:11

Page 13 of 14

Franceschini S, Fedkenheuer M, Vogelaar NJ, Robinson HH, Sobrado P, Mattevi A (2012) Structural insight into the mechanism of oxygen activation and substrate selectivity of flavin-dependent N-hydroxylating monooxygenases. Biochemistry 51(36):7043–7045

Ganz T (2009) Iron in innate immunity: starve the invaders. Curr Opin Immunol 21(1):63–67

Ganz T (2016) Macrophages and iron metabolism. Microbiol Spectr 4(5):1–10

Ganz T (2018) Iron and infection. Int J Hematol 107(1):7–15

Geromanos SJ, Vissers JP, Silva JC, Dorschel CA, Li GZ, Gorenstein MV et al (2009) The detection, correlation, and comparison of peptide precursor and product ions from data independent LC-MS with data dependant LC-MS/MS. Proteomics 9(6):1683–1695

Haas H (2003) Molecular genetics of fungal siderophore biosynthesis and uptake: the role of siderophores in iron uptake and storage. Appl Microbiol Biotechnol 62(4):316–330

Haas H, Schoeser M, Lesuisse E, Ernst JF, Parson W, Abt B et al (2003) Characterization of the *Aspergillus nidulans* transporters for the siderophores enterobactin and triacetylfusarinine C. Biochem J 371(Pt 2):505–513

Haas H, Zadra I, Stoffler G, Angermayr K (1999) The *Aspergillus nidulans* GATA factor SREA is involved in regulation of siderophore biosynthesis and control of iron uptake. J Biol Chem 274(8):4613–4619

Haber F, Weiss J (1934) The catalytic decomposition of hydrogen peroxide by iron salts. Proc Royal Soc London 147:332–351

Halliwell B, Gutteridge JM (1984) Oxygen toxicity, oxygen radicals, transition metals and disease. Biochem J 219(1):1–14

Hernandez O, Almeida AJ, Gonzalez A, Garcia AM, Tamayo D, Cano LE et al (2010) A 32-kilodalton hydrolase plays an important role in *Paracoccidioides brasiliensis* adherence to host cells and influences pathogenicity. Infect Immun 78(12):5280–5286

Heymann P, Gerads M, Schaller M, Dromer F, Winkelmann G, Ernst JF (2002) The siderophore iron transporter of *Candida albicans* (Sit1p/Arn1p) mediates uptake of ferrichrome-type siderophores and is required for epithelial invasion. Infect Immun 70(9):5246–5255

Hilty J, George Smulian A, Newman SL (2011) *Histoplasma capsulatum* utilizes siderophores for intracellular iron acquisition in macrophages. Med Mycol 49(6):633–642

Hwang LH, Mayfield JA, Rine J, Sil A (2008) *Histoplasma* requires *SID1*, a member of an iron-regulated siderophore gene cluster, for host colonization. PLoS Pathog 4(4):e1000044

Jorjao AL, Oliveira LD, Scorzoni L, Figueiredo-Godoi LMA, Cristina APM, Jorge AOC et al (2018) From moths to caterpillars: ideal conditions for *Galleria mellonella* rearing for in vivo microbiological studies. Virulence 9(1):383–389

Kalidasan V, Azman A, Joseph N, Kumar S, Awang Hamat R, Neela VK (2018) Putative iron Acquisition Systems in *Stenotrophomonas maltophilia*. Molecules 23(8):2048

Kornitzer D (2009) Fungal mechanisms for host iron acquisition. Curr Opin Microbiol 12(4):377–383

Kosman DJ (2003) Molecular mechanisms of iron uptake in fungi. Mol Microbiol 47(5):1185–1197

Krithika R, Marathe U, Saxena P, Ansari MZ, Mohanty D, Gokhale RS (2006) A genetic locus required for iron acquisition in *Mycobacterium tuberculosis*. Proc Natl Acad Sci U S A 103(7):2069–2074

Lima Pde S, Chung D, Bailao AM, Cramer RA, Soares CM (2015) Characterization of the *Paracoccidioides* hypoxia response reveals new insights into pathogenesis mechanisms of this important human pathogenic fungus. PLoS Negl Trop Dis 9(12):e0004282

Machuca A, Milagres AM (2003) Use of CAS-agar plate modified to study the effect of different variables on the siderophore production by *Aspergillus*. Lett Appl Microbiol 36(3):177–181

Marcos CM, de Silva JF, Oliveira HC, Assato PA, Singulani Jde L, Lopez AM et al (2016) Decreased expression of 14-3-3 in *Paracoccidioides brasiliensis* confirms its involvement in fungal pathogenesis. Virulence 7(2):72–84

Marcos CM, Tamer G, de Oliveira HC, Assato PA, Scorzoni L, Santos CT et al (2019) Down-regulation of TUFM impairs host cell interaction and virulence by *Paracoccidioides brasiliensis*. Sci Rep 9(1):17206

McDonagh A, Fedorova ND, Crabtree J, Yu Y, Kim S, Chen D et al (2008) Sub-telomere directed gene expression during initiation of invasive aspergillosis. PLoS Pathog 4(9):e1000154

McEwen JG, Bedoya V, Patino MM, Salazar ME, Restrepo A (1987) Experimental murine paracoccidiodomycosis induced by the inhalation of conidia. J Med Vet Mycol 25(3):165–175

Menino JF, Almeida AJ, Rodrigues F (2012) Gene knockdown in *Paracoccidioides brasiliensis* using antisense RNA. Methods Mol Biol 845:187–198

Murad AM, Souza GH, Garcia JS, Rech EL (2011) Detection and expression analysis of recombinant proteins in plant-derived complex mixtures using nanoUPLC-MS(E). J Sep Sci 34(19):2618–2630

Neilands JB (1993) Siderophores. Arch Biochem Biophys 302(1):1–3

Nevitt T, Thiele DJ (2011) Host iron withholding demands siderophore utilization for *Candida glabrata* to survive macrophage killing. PLoS Pathog 7(3): e1001322

Nogueira SV, Fonseca FL, Rodrigues ML, Mundoi V, Abi-Chacra EA, Winters MS et al (2010) *Paracoccidioides brasiliensis* enolase is a surface protein that binds plasminogen and mediates interaction of yeast forms with host cells. Infect Immun 78(9):4040–4050

Parente AF, Bailao AM, Borges CL, Parente JA, Magalhaes AD, Ricart CA et al (2011) Proteomic analysis reveals that iron availability alters the metabolic status of the pathogenic fungus *Paracoccidioides brasiliensis*. PLoS One 6(7): e22810

Parente-Rocha JA, Parente AF, Baeza LC, Bonfim SM, Hernandez O, McEwen JG et al (2015) Macrophage interaction with *Paracoccidioides brasiliensis* yeast cells modulates fungal metabolism and generates a response to oxidative stress. PLoS One 10(9):e0137619

Pasricha S, Schafferer L, Lindner H, Joanne Boyce K, Haas H, Andrianopoulos A (2016) Differentially regulated high-affinity iron assimilation systems support growth of the various cell types in the dimorphic pathogen *Talaromyces marneffei*. Mol Microbiol 102(4):715–737

Perez-Miranda S, Cabirol N, George-Tellez R, Zamudio-Rivera LS, Fernandez FJ (2007) O-CAS, a fast and universal method for siderophore detection. J Microbiol Methods 70(1):127–131

Philpott CC, Protchenko O (2008) Response to iron deprivation in *Saccharomyces cerevisiae*. Eukaryot Cell 7(1):20–27

Pronk S, Pall S, Schulz R, Larsson P, Bjelkmar P, Apostolov R et al (2013) GROMACS 4.5: a high-throughput and highly parallel open source molecular simulation toolkit. Bioinformatics 29(7):845–854

Raymond KN, Dertz EA, Kim SS (2003) Enterobactin: an archetype for microbial iron transport. Proc Natl Acad Sci U S A 100(7):3584–3588

Restrepo A (1985) The ecology of *Paracoccidioides brasiliensis*: a puzzle still unsolved. Sabouraudia 23(5):323–334

Restrepo A, Jimenez BE (1980) Growth of *Paracoccidioides brasiliensis* yeast phase in a chemically defined culture medium. J Clin Microbiol 12(2):279–281

Restrepo A, McEwen JG, Castaneda E (2001) The habitat of *Paracoccidioides brasiliensis*: how far from solving the riddle? Med Mycol 39(3):233–241

Rezende TC, Borges CL, Magalhaes AD, de Sousa MV, Ricart CA, Bailao AM et al (2011) A quantitative view of the morphological phases of *Paracoccidioides brasiliensis* using proteomics. J Proteomics 75(2):572–587

Rigsby RE, Parker AB (2016) Using the PyMOL application to reinforce visual understanding of protein structure. Biochem Mol Biol Educ 44(5):433–437

Robinson R, Franceschini S, Fedkenheuer M, Rodriguez PJ, Ellerbrock J, Romero E et al (2014) Arg279 is the key regulator of coenzyme selectivity in the flavin-dependent ornithine monooxygenase SidA. Biochim Biophys Acta 1844(4): 778–784

Robinson R, Qureshi IA, Klancher CA, Rodriguez PJ, Tanner JJ, Sobrado P (2015) Contribution to catalysis of ornithine binding residues in ornithine N5-monooxygenase. Arch Biochem Biophys 585:25–31

San-Blas G, Nino-Vega G, Iturriaga T (2002) *Paracoccidioides brasiliensis* and paracoccidioidomycosis: molecular approaches to morphogenesis, diagnosis, epidemiology, taxonomy and genetics. Med Mycol 40(3):225–242

Sanchez M, Sabio L, Galvez N, Capdevila M, Dominguez-Vera JM (2017) Iron chemistry at the service of life. IUBMB Life 69(6):382–388

Schneider CA, Rasband WS, Eliceiri KW (2012) NIH image to ImageJ: 25 years of image analysis. Nat Methods 9(7):671–675

Schrettl M, Bignell E, Kragl C, Joechl C, Rogers T, Arst HN Jr et al (2004) Siderophore biosynthesis but not reductive iron assimilation is essential for *Aspergillus fumigatus* virulence. J Exp Med 200(9):1213–1219

Schrettl M, Bignell E, Kragl C, Sabiha Y, Loss O, Eisendle M et al (2007) Distinct roles for intra- and extracellular siderophores during *Aspergillus fumigatus* infection. PLoS Pathog 3(9):1195–1207

Schrettl M, Ibrahim-Granet O, Droin S, Huerre M, Latge JP, Haas H (2010) The crucial role of the *Aspergillus fumigatus* siderophore system in interaction with alveolar macrophages. Microbes Infect 12(12–13):1035–1041

Schwyn B, Neilands JB (1987) Universal chemical assay for the detection and determination of siderophores. Anal Biochem 160(1):47–56

Scorzoni L, de Paula e Silva AC, de Singulani JL, Leite FS, de Oliveira HC, da Silva RA et al (2015) Comparison of virulence between *Paracoccidioides brasiliensis* and *Paracoccidioides lutzii* using *Galleria mellonella* as a host model. Virulence 6(8):766–776

Silva APRV, A. D, Viana RO, Ricoy A, C. DS, Johann S, Alves VDS (2018) *Caenorhabditis elegans* and *Tenebrio molitor* - new tools to investigate *Malassezia species* Preprints 1

Silva MG, Schrank A, Bailao EF, Bailao AM, Borges CL, Staats CC et al (2011) The homeostasis of iron, copper, and zinc in *Paracoccidioides brasiliensis*, *Cryptococcus neoformans* var. *grubii*, and *Cryptococcus gattii*: a comparative analysis. Front Microbiol 2:49

Silva-Bailao MG, Bailao EF, Lechner BE, Gauthier GM, Lindner H, Bailao AM et al (2014) Hydroxamate production as a high affinity iron acquisition mechanism in *Paracoccidioides* spp. PLoS One 9(8):e105805

Thomaz L, Garcia-Rodas R, Guimaraes AJ, Taborda CP, Zaragoza O, Nosanchuk JD (2013) Galleria mellonella as a model host to study *Paracoccidioides lutzii* and *Histoplasma capsulatum*. Virulence 4(2):139–146

Tomazett MV, Baeza LC, Paccez JD, Parente-Rocha JA, Ribeiro-Dias F, Soares CMA (2019) Identification and characterization of *Paracoccidioides lutzii* proteins interacting with macrophages. Microbes Infect S1286–4579(19):30046–30042[pii]. https://doi.org/10.1016/j.micinf.2019.03.002

Vargas G, Rocha JD, Oliveira DL, Albuquerque PC, Frases S, Santos SS et al (2015) Compositional and immunobiological analyses of extracellular vesicles released by *Candida albicans*. Cell Microbiol 17(3):389–407

Wilson-Sanders SE (2011) Invertebrate models for biomedical research, testing, and education. ILAR J 52(2):126–152

Yang J, Zhang Y (2015) Protein structure and function prediction using I-TASSER. Curr Protoc Bioinformatics 52:581–515

Zambuzzi-Carvalho PF, Tomazett PK, Santos SC, Ferri PH, Borges CL, Martins WS et al (2013) Transcriptional profile of *Paracoccidioides* induced by oenothein B, a potential antifungal agent from the Brazilian Cerrado plant Eugenia uniflora. BMC Microbiol 13:227

Zhou LW, Haas H, Marzluf GA (1998) Isolation and characterization of a new gene, sre, which encodes a GATA-type regulatory protein that controls iron transport in *Neurospora crassa*. Mol Gen Genet 259(5):532–540

Publisher's Note